PHASE RELATIONS AND STABILITY STUDIES IN THE Si_3N_4-SiO_2-Y_2O_3 PSEUDO-TERNARY SYSTEM

WESTINGHOUSE ELECTRIC CORPORATION

PREPARED FOR
OFFICE OF NAVAL RESEARCH

1 APRIL 1976

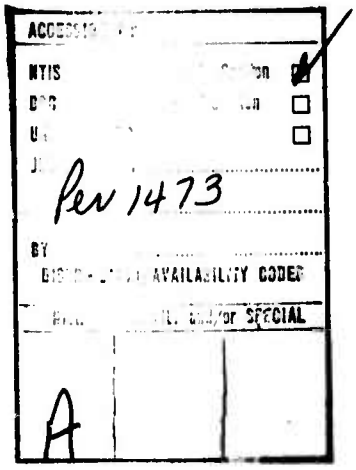

PHASE RELATIONS AND STABILITY STUDIES IN THE Si_3N_4-SiO_2-Y_2O_3 PSEUDO-TERNARY SYSTEM

F. F. Lange, S. C. Singhal and R. C. Kuznicki

Technical Report #6, April 1, 1976

Westinghouse Electric Corporation
Research and Development Center

Contract Number N00014-74-C-0284

Sponsored by the Advanced Projects Agency
ARPA Order Number 2697
Program Code Number 01269

Scientific Officer: Dr. A. M. Diness
Office of Naval Research

Principal Investigator: Dr. F. F. Lange
(412) 256-3684

Effective Date of Contract: April 1, 1974

Contract Expiration Date: June 30, 1976

Amount of Contract: $159,892

Form Approved, Budget -- No. 22-R0293

Unclassified

SECURITY CLASSIFICATION OF THIS PAGE (When Data Entered)

REPORT DOCUMENTATION PAGE		READ INSTRUCTIONS BEFORE COMPLETING FORM
1. REPORT NUMBER	2. GOVT ACCESSION NO.	3. RECIPIENT'S CATALOG NUMBER
4. TITLE (and Subtitle) PHASE RELATIONS AND STABILITY STUDIES IN THE Si_3N_4-SiO_2-Y_2O_3 PSEUDO-TERNARY SYSTEM		5. TYPE OF REPORT & PERIOD COVERED Technical Report #6 April 1, 1976 6. PERFORMING ORG. REPORT NUMBER
7. AUTHOR(s) F.F. Lange, S.C. Singhal and R.C. Kuznicki		8. CONTRACT OR GRANT NUMBER(s) N00014-74-C-0284
9. PERFORMING ORGANIZATION NAME AND ADDRESS Westinghouse Research & Development Center Pittsburgh, Pennsylvania 15235		10. PROGRAM ELEMENT, PROJECT, TASK AREA & WORK UNIT NUMBERS
11. CONTROLLING OFFICE NAME AND ADDRESS		12. REPORT DATE April 1, 1976 13. NUMBER OF PAGES 23
14. MONITORING AGENCY NAME & ADDRESS(if different from Controlling Office)		15. SECURITY CLASS. (of this report) Unclassified 15a. DECLASSIFICATION DOWNGRADING SCHEDULE

16. DISTRIBUTION STATEMENT (of this Report)

Reproduction in whole or in part is permitted for any purpose of the U.S. Government. Distribution of this document is UNLIMITED.

17. DISTRIBUTION STATEMENT (of the abstract entered in Block 20, if different from Report)

18. SUPPLEMENTARY NOTES

19. KEY WORDS (Continue on reverse side if necessary and identify by block number)

silicon nitride, oxidation, yttrium oxide, hot, phase, stability, pressing

20. ABSTRACT (Continue on reverse side if necessary and identify by block number)

Composite powders were hot-pressed to determine the phase relations within the Si_3N_4-SiO_2-Y_2O_3 pseudo-ternary system. Four quaternary compounds, viz., $Si_3Y_2O_3N_4$, $YSiO_2N$, $Y_{10}Si_7O_{23}N_4$ and $Y_4Si_2O_7N_2$ were identified. Studies of polyphase and single-phase materials within this system showed that these four compounds were unstable under oxidizing conditions. Materials within

DD FORM 1 JAN 73 1473 EDITION OF 1 NOV 65 IS OBSOLETE

Unclassified

SECURITY CLASSIFICATION OF THIS PAGE (When Data Entered)

20. (Cont'd)

the Si_3N_4-Si_2N_2O-$Y_2Si_2O_7$ compatibility triangle precluded the unstable compounds, and these materials were found to be extremely resistant to oxidation.

Research Report 76-9D4-POWDR-R1
Proprietary Class Unrestricted

April 1, 1976

PHASE RELATIONS AND STABILITY STUDIES IN THE Si_3N_4-SiO_2-Y_2O_3 PSEUDO-TERNARY SYSTEM

F. F. Lange, S. C. Singhal and R. C. Kuznicki
Metallurgy and Metals Processing

Westinghouse Research Laboratories
Pittsburgh, Pennsylvania 15235

ABSTRACT

Composite powders were hot-pressed to determine the phase relations within the Si_3N_4-SiO_2-Y_2O_3 pseudo-ternary system. Four quaternary compounds, viz., $Si_3Y_2O_3N_4$, $YSiO_2N$, $Y_{10}Si_7O_{23}N_4$ and $Y_4Si_2O_7N_2$ were identified. Studies of polyphase and single-phase materials within this system showed that these four compounds were unstable under oxidizing conditions. Materials within the Si_3N_4-Si_2N_2O-$Y_2Si_2O_7$ compatibility triangle precluded the unstable compounds, and these materials were found to be extremely resistant to oxidation.

1. INTRODUCTION

The use of Y_2O_3 as a hot-pressing aid to densify Si_3N_4 powder has been discussed by a number of investigators.[1,2,3,4] Preliminary property measurements at temperatures > 1300°C reported by Gazza[1] indicated that Si_3N_4 densified with Y_2O_3 had significantly improved high temperature mechanical properties relative to Si_3N_4 densified with the more conventional hot-pressing aid, MgO. The initial results of the present workers were in agreement with the general conclusions of Gazza until it was found that some of the Si_3N_4-Y_2O_3 type materials were unstable at intermediate temperatures (~1000°C) despite their apparent stability at 1400°C.

Preliminary experiments designed to investigate this unusual phenomenon suggested that at least one of the secondary phases in these materials, viz., $Si_3Y_2O_3N_4$, was unstable in oxidizing environments. Further experiments were designed to fabricate $Si_3Y_2O_3N_4$ as a single phase material to examine its oxidation behavior. In addition, the phase relations in the Si_3N_4-SiO_2-Y_2O_3 system were examined to determine whether a tie line existed which would preclude the presence of the unstable phases in the hot-pressed materials.

As discussed below, four Si-Y-O-N compounds were found to readily oxidize. However, materials fabricated within the Si_3N_4-$Y_2Si_2O_7$-Si_2N_2O compatibility triangle precluded these unstable compounds and they exhibited the best oxidation resistance of any of the hot-pressed Si_3N_4 materials examined to date.

2. EXPERIMENTAL

2.1 Powders, Preparation and Fabrication

The cation impurities of the Si_3N_4*, SiO_2** and Y_2O_3*** powders used in this study are shown in Table 1. The Si_3N_4 powder contained ∿90% α-Si_3N_4, ∿10% β-Si_3N_4, 1% free Si and 0.7 wt% oxygen as determined with the inert gas fusion, thermoconductivity method. Only those portions of the phase diagram were examined that did not require YN as a starting constituent.

The selected powder compositions were prepared for fabrication by milling in a polyethylene bottle with WC media and methanol. Weight measurements of the milling media and the container, both before and after milling, showed that the WC and plastic contamination in the milled powders were in the range of 1.5-3 wt% and 0.7-1.5 wt%, respectively.

Prepressed discs of the composite powders were hot-pressed in a 5 cm I.D. graphite die-susceptor lined with grafoil† at a pressure of 28 MN/m^2, and temperatures between 1600°C and 1780°C as measured with an optical pyrometer. The maximum temperature was maintained for two hours before the power to the furnace was shut off. Densification was monitored with a sliding-resistance indicator. A nitrogen atmosphere was maintained within the furnace chamber. In a few cases, the liquidus temperature of a particular composition was exceeded. Such compositions were hot-pressed again at a lower temperature.

After sandblasting the density of each hot-pressed disc was determined by water immersion, a specimen of each hot-pressed composition was ground to a fine powder (-200 mesh) to determine the crystalline phases by x-ray diffraction.

---

*Westinghouse Research Laboratories, Pittsburgh, Pennsylvania 15235.

**Fisher Scientific Company, New Jersey 07410.

***Research Chemicals, Phoenix, Arizona 85031.

†Union Carbide, Carbon Products Division, New York 10017.

2.2 Oxidation Experiments

The stability of each hot-pressed composition in air at 1000°C was investigated by placing diamond-cut rectangular specimens, supported on two knife-edged triangular prisms of hot-pressed NC 132 Si_3N_4*, inside an open-ended muffle tube of a resistance heated furnace. Weight changes of the specimens were periodically measured. Some compositions were exposed over 1000 hrs; others had to be removed after a short period due to severe cracking and/or crumbling. Specific compositions were also examined in a similar manner at 1375°C. Phases present before and after oxidation were determined by x-ray diffraction.

The oxidation behavior of $Si_3Y_2O_3N_4$ was investigated with continuous thermogravimetry using an automatic Cahn electrobalance between 1000°C and 1320°C in pure oxygen, air, and argon. The experimental procedure and details of specimen dimensions are described elsewhere.[5] The concentration of Y, Si and O across the oxide scale on $Si_3Y_2O_3N_4$ were determined using an electron microprobe. The morphology of the oxide scale was examined with a scanning electron microscope.

3. RESULTS AND OBSERVATIONS

3.1 Phase Relations

Hot-pressed compositions containing > 90 mole % Si_3N_4 contained some (0 to 12%) open porosity, as determined by water absorption. Other compositions did not contain porosity. All compositions exhibited a weight loss of 3 to 10% after fabrication. Compositions exhibiting weight losses $\geq$ 10% were fabricated again at a lower temperature. Some of the weight loss was caused by a reaction with the graphite liner resulting in a friable SiC product which was removed by sandblasting. Other suspected causes for weight loss are the loss of the plastic contaminant, the loss of absorbed water, and the loss of Si_3N_4 and SiO_2 due to decomposition and

*Norton Co., Worcester, Massachusetts 01606.

volatilization as SiO vapor, respectively. The final compositions of the hot-pressed discs were not determined, but the possibility of small compositional changes during fabrication should not alter the general conclusions of this work.

Densification measurements were insufficient to indicate solidus temperatures. No attempt was made to define the liquidus temperatures in the present study.

The compositions examined are shown in Fig. 1 as solid circles along with the resulting phase relations. Tungsten carbide was also detected in every hot-pressed composition. Phase areas without solid circles were not investigated.

Identification of $Y_2Si_2O_7$ was made with reference to Ito and Johnston[6] and Batelieva, et al.[7] The five polymorphic structures of $Y_2Si_2O_7$ made initial identification of this compound difficult. The γ structure of $Y_2Si_2O_7$ was only observed in the Si_3N_4-$Y_{10}Si_7O_{23}N_4$-$Y_2Si_2O_7$ compatibility triangle, whereas only the low temperature α-structure was observed in the Si_3N_4-Si_2N_2O-$Y_2Si_2O_7$ compatibility triangle. Oxidation studies, described below, lead to other structures of $Y_2Si_2O_7$ depending on the oxidation temperature. The compound Y_2SiO_5 was identified with ASTM card 21-1458. It should be pointed out that the diffraction patterns reported by Toropov and Bondar,[8] who determined the Y_2O_3-SiO_2 phase diagram, bear no resemblance to patterns reported by others.

The x-ray diffraction patterns for $Si_3Y_2O_3N_4$,[2,4,9] J-phase[4,9] and H-phase[4,9] have been reported by others. Tsuge et al.,[4] Wills[9] and the present workers are in agreement with the existence of $Si_3Y_2O_3N_4$. The J-phase was interpreted as $Y_4Si_3O_6N_4$ ($2Y_2O_3 \cdot Si_3N_4$) by Tsuge et al.,[2] and as $Y_6Si_3O_9N_4$ ($3Y_2O_3 \cdot Si_3N_4$) by both Rae, et al.[4] and Wills.[9] Recent work by Morgan[10] has suggested that the J-phase is $Y_4Si_2O_7N_2$ ($2Y_2O_3 \cdot Si_2N_2O$), which is consistent with the observations of the present workers. Rae et al.[4] have suggested that the H-phase is $Y_5Si_3O_{12}N$ ($10Y_2O_3 \cdot 9SiO_2 \cdot Si_3N_4$). However, the present workers find that the repeated fabrication of this composition results in two phases,* viz., H-phase and

*Hamon et al.,[11] who have synthesized many apatite-like, $Ln_5Si_3O_{12}N$ Ln = Sm, La, Nd, Sm, Gd) compounds were also unable to synthesize $Y_5Si_3O_{12}N$.

Y_2SiO_5 and as shown in Fig. 1, the present workers represent the H-phase with the composition of $Y_{10}Si_7O_{23}N_4$ ($5Y_2O_3 \cdot 4SiO_2 \cdot Si_3N_4$).

Small differences were observed between the diffraction patterns of the above three compounds reported by others and those observed by the present workers shown in Table 2. These differences may be a result of either unidentified solid-solution in these three compositional areas or the solid-solution with the impurities present in the initial powders. It is believed that the Si_3N_4 powder used by the present workers was purer than those used by others.*

For polyphase materials within this system, no change in the Si_3N_4 diffraction pattern was observed. This indicated that Y is not soluble in the Si_3N_4 structures in contrast to that observed for Al[13] and Be[14].

Table III shows the observed x-ray diffraction data for the K-phase, which has not been reported by others. Repeated fabrication indicates a composition of $YSiO_2N$ ($Y_2O_3 \cdot Si_2N_2O$). Good agreement was obtained when these data were indexed[15] on the basis of a monoclinic unit cell with lattice parameters a = 9.208 Å, b = 13.157 Å, c = 8.675 Å and β = 97.471 Å. The measured density of 4.276 g/cm^3 for this compound is in good agreement with the calculated density of 4.158 g/cm^2 (16 $YSiO_2N$ molecules/unit cell) when the WC contamination is considered.

3.2 Oxidation

3.2.1 Polyphase Materials in the Si_3N_4-$Y_2Si_2O_7$-Y_2O_3 Phase Area

All dense polyphase materials within the Si_3N_4-$Y_2Si_2O_7$-Y_2O_3 phase area exhibited relatively large weight gains in air environments at 1000°C. Compositions closer to the four quaternary phases ($Si_3Y_2O_3N_4$, K, H and J) exhibited greater weight gains than those closer to other members of this phase area as illustrated in Fig. 2 for the compositions

*Others fail to report impurity contents and they apparently fail to include the high SiO_2 content of commercial Si_3N_4 powders (up to 12 mole %)[12]

a, b, c and d (see Fig. 1), which were oxidized in air for 20 hrs at 1000°C. As shown, weight gain increases with increasing $Si_3Y_2O_3N_4$ content.

The development of large cracks, and in many cases, the complete disintegration of the previously dense, rectangular specimen into a friable mass as illustrated in Fig. 3 (composition d, 20 hrs, 1000°C), was concurrent with the observed weight gains.

X-ray diffraction analysis revealed that the four quaternary phases originally present in the polyphase materials disappeared after extended periods of oxidation at 1000°C and that SiO_2 (crystobilite), a yttrium silicate and β-Si_3N_4 were the phases present in the oxidized materials. As shown below, the different quaternary phases oxidized to different yttrium silicates. In addition, the trace amounts of WC also disappeared during oxidation.

Several polyphase materials in the Si_3N_4-$YSiO_2N$-$Si_3Y_2O_3N_4$ compatibility triangle were oxidized in air at 1375°C for periods up to 300 hrs. Much smaller weight gains were recorded at 1375°C than at 1000°C, e.g., the weight of composition d (see Fig. 1) only increased by 0.37 mg/cm^2 after 114 hrs and exhibited no cracking, etc. at 1375°C, as compared to much larger weight gain and its degradation at 1000°C illustrated in Fig. 2 and Fig. 3, respectively. X-ray analysis of the glassy appearing oxide surface layer formed on this composition after exposure at 1375°C for 100 hrs revealed only $Y_2Si_2O_7$ and SiO_2.

Specimens of composition d (see Fig. 1) pre-oxidized at 1375°C for 100 hrs and then placed in a furnace at 1000°C exhibited ~1/10 the total weight gain exhibited by specimens exposed for similar periods without the pre-oxidation treatment. Eventually this and similar pre-oxidized polyphase materials did exhibit cracking similar to the same materials without the pre-oxidation treatment. These results strongly suggest that the surface oxide layer formed at 1375°C retarded the further oxidation at both 1375°C and 1000°C.

3.2.2 Polyphase Materials in the Si_3N_4-Si_2N_2O-$Y_2Si_2O_7$ Compatibility Triangle

The weight changes of the dense materials within this compatibility triangle exposed to air at 1000°C were negligible and within the error of measurement (± 0.0005 gm), e.g., composition e (see Fig. 1) exposed to air at 1000°C for 1000 hrs exhibited a weight gain of only 0.01%.

Weight gained by these materials at 1375°C was also small, e.g., composition e exposed for a period of 303 hrs exhibited a weight gain of only 0.21 mg/cm^2. An x-ray diffraction analysis of the oxide layer formed on this specimen revealed that SiO_2 was the only crystalline phase formed by oxidation at this temperature.

3.2.3 Single Phase Materials

3.2.3.1 $Si_3Y_2O_3N_4$

This is the only material that was studied using an automatic electrobalance. Specimens of $Si_3Y_2O_3N_4$ exposed to one atmosphere of flowing (.4 l/min), purified argon gas at 1000°C did not change weight for exposure periods up to 72 hrs. Large weight gains were recorded in both purified oxygen and air environments (flow rate = 0.4 l/min) at 1000°C, 1200°C and 1300°C as shown in Fig. 4. It is clear from these data that the weight gains exhibited by $Si_3Y_2O_3N_4$ in oxidizing environments increased linearly with time at all temperatures.

One $Si_3Y_2O_3N_4$ specimen was oxidized in oxygen at 1320°C until its weight became constant. The total weight gain was found to be consistent with the complete conversion of $Si_3Y_2O_3N_4$ to $Y_2Si_2O_7$ and SiO_2 according to the reaction

$$Si_3Y_2O_3N_4 + 3O_2 \rightarrow Y_2Si_2O_7 + SiO_2 + 2N_2 \ . \qquad (1)$$

X-ray diffraction analysis showed that the y-structure of $Y_2Si_2O_7$ formed at 1000°C, whereas the γ-structure formed at 1320°C, consistent with the structure-temperature observations of Ito and Johnston[6].

The thick scale formed on $Si_3Y_2O_3N_4$ after exposure to air at 1000°C is illustrated in Fig. 5. The SEM micrograph in this figure shows the presence of many small cracks in the oxide scale. Electron microprobe traces for Y, Si and O across the $Si_3Y_2O_3N_4$ substrate-scale interface showed that the scale had an increased O content relative to the substrate.

3.2.3.2 Other Quaternary Phases

The other quaternary phases also readily oxidized and became friable masses when exposed to air at 1000°C for periods $\leq$ 50 hrs. The observed products of oxidation at 1000°C suggest the following reactions:

$$2YSiO_2N \text{ (K-phase)} + 1.5\ O_2 \rightarrow Y_2Si_2O_7 + N_2 \qquad (2)$$

$$Y_{10}Si_7O_{23}N_4 \text{ (H-phase)} + 3O_2 \rightarrow 5Y_2SiO_5 + 2SiO_2 + 2N_2 \qquad (3)$$

$$Y_4Si_2O_7N_2 \text{ (J-phase)} + 1.5O_2 \rightarrow 2Y_2SiO_5 + N_2 \qquad (4)$$

4. DISCUSSION

4.1 Oxidation

It is clear from the data presented that the four quaternary compounds readily oxidize when exposed to an oxidizing environment at high temperatures. Moreover, unlike Si_3N_4, which exhibits parabolic oxidation kinetics, $Si_3Y_2O_3N_4$ (and more than likely, the other three quaternary compounds) exhibits linear oxidation kinetics. The linear oxidation kinetics indicates the formation of a non-protective, porous oxide scale over $Si_3Y_2O_3N_4$. The porous nature of the oxide and the presence of large numbers of cracks in it are evident in the scanning electron micrograph in Fig. 5.

In the case of metals, one of the several possible reasons that porous scales are formed on oxidation is that the molar volume of

the oxide is smaller than that of the metal itself,[16] so that the oxide does not cover the entire surface of the metal. It appears that in the oxidation of the four quaternary compounds in the Si_3N_4-SiO_2-Y_2O_3 system, the volume of the oxide formed is less than the volume of the Si-Y-O-N compound itself which causes the formation of non-protective porous oxide on the surface. For example, in the oxidation of $Si_3Y_2O_3N_4$, most likely the initial oxidation product is $Y_2O_3 \cdot SiO_2$, which then combines with SiO_2 to form $Y_2O_3 \cdot 2SiO_2$. The densities of $Si_3Y_2O_3N_4$ and $Y_2O_3 \cdot SiO_2$ are reported as 4.28[2] and 4.49[17] g cm^{-3}, respectively, indicating the molar volume of the $Y_2O_3 \cdot SiO_2$ oxide to be smaller than that of the $Si_3Y_2O_3N_4$. In addition to these volume differences, the fact that a mixture of two oxides are formed by oxidation according to reactions (1) and (3) could also result in the formation of porous oxide scales due to differences in their nucleation and growth morphologies.[18]

The most unusual oxidation phenomenon observed here was the relative stability of certain polyphase materials at 1375°C, but their degradation at 1000°C. This phenomenon can be explained by suggesting that the compact protective SiO_2 surface layer formed over Si_3N_4 in such materials at high temperatures (e.g., 1375°C) retarded or eliminated the oxidation of the unstable phases. At lower temperatures (e.g., 1000°C), it has been found that Si_3N_4 does not exhibit much oxidation,[5] so that the SiO_2 surface layer would be insufficient to completely cover the unstable phase. Thus, at lower temperatures, the unstable phases could oxidize, causing internal stresses to build up, resulting in eventual cracking and disintegration of the specimen. This reasoning also explains the relatively greater oxidation-resistance of the pre-oxidized specimens at the lower temperatures.

The excellent oxidation resistance of materials fabricated within the Si_3N_4-Si_2N_2O-$Y_2Si_2O_7$ compatibility triangle can be explained by examining the phase equilibria between SiO_2 (the oxidation product of either Si_3N_4 or Si_2N_2O) and $Y_2Si_2O_7$. As shown in Fig. 1 and in the

SiO_2-Y_2O_3 phase diagram reported by Toropov and Bondar,[8] both SiO_2 and $Y_2Si_2O_7$ can exist in equilibrium with one another. Until the eutectic temperature (1660°C) between these two phases is reached, no reaction or interdiffusion between these two phases should take place. Thus, at temperatures below 1660°C, materials within this compatibility triangle exhibit oxidation kinetics intrinsic to either Si_3N_4 or Si_2N_2O, and, therefore, extremely good resistance to oxidation.

4.2 Densification

Although eutectic and liquidus temperatures were not determined in this study, it is reasonable to suggest that a liquid phase is responsible for densification within this and other similar systems. When a given composition is hot-pressed from a mixture of Si_3N_4, SiO_2 and Y_2O_3, a liquid will first form at the lowest eutectic temperature within this system. As reaction proceeds, the volume fraction of the liquid will eventually be governed by the solidus and the liquidus temperatures of the compatibility triangle containing the chosen composition. Thus, future densification studies should include the determination of eutectic and liquidus temperatures.

4.3 Summary

Dense materials fabricated within the Si_3N_4-Si_2N_2O-$Y_2Si_2O_7$ compatibility triangle are extremely stable in oxygen environments relative to other silicon-nitrogen ceramics. Preliminary property measurements indicate that some compositions within this compatibility triangle will be useful, high temperature structural materials. Other materials in the Si_3N_4-SiO_2-Y_2O_3 system were found to be prone to accelerated oxidation in high temperature environments due to the instability of four quaternary compounds.

ACKNOWLEDGMENTS

The authors thank the technical assistance of J. J. Nalevanko, T. A. Manion and J. A. Fraino, and the special help of G. G. Johnson, Jr. of the Pennsylvania State University who made the indexing program available. This work was supported by the Advanced Research Projects Agency and monitored by the Office of Naval Research, Contract No. N00014-74-C-0284.

BIBLIOGRAPHY

1. G. E. Gazza, "Effect of Y_2O_3 Additions on Hot-Pressed Si_3N_4," Bul. Amer. Ceram. Soc. 54 [9] 778-81 (1975).

2. A. Tsuge, H. Kudo and K. Komeya, "Reaction of Si_3N_4 and Y_2O_3 in Hot-Pressing," J. Amer. Ceram. Soc. 57 [6] 269-70 (1974).

3. A. Tsage, K. Nishida and M. Komatsu, "Effect of Crystallizing the Grain Boundary Phase on the High-Temperature Strength of Hot-Pressed Si_3N_4 Containing Y_2O_3," J. Amer. Ceram. Soc. 58 [7] 323 (1975).

4. A. N. J. M. Rae, D. P. Thompson, N. J. Pipkin and K. H. Jack, "The Structure of Yttrium Silicon Oxynitride and its Role in the Hot-Pressing of Si_3N_4 with Y_2O_3 Additions," Special Ceramics, Vol. 6, Ed. by P. Popper, pp. 347-60, B.C.R.A. Stoke-on-Trent (1975).

5. S. C. Singhal, "Thermodynamics and Kinetics of Oxidation of Hot-Pressed Si_3N_4," J. Mat. Sci. 11, 500-9 (1976).

6. J. Ito and H. Johnson, "Synthesis and Study of Yttrialite," Amer. Min. 53 (1968).

7. N. G. Batalieva, I. A. Bondar, G. A. Sidorenko and N. A. Toropov, "Synthetic Silicate $Y_2Si_2O_7$," Doklady Akademi Nank SSSR, 173 [2], 339-41 (1967) (Eng. Trans.).

8. N. A. Toropov and I. A. Bondar, "Phase Diagram of the Binary System: Y_2O_3-SiO_2," Izvesiya Akad. Nank SSSR, Otdelente Khimicheskh Nank No. 4, 544-50 (1961) (Eng. Trans.).

9. R. R. Wills, "Silicon Yttrium Oxynitride," J. Amer. Ceram. Soc. 57, 459 (1974).

10. P. E. D. Morgan, "Comment on 'Reaction of Si_3N_4 with Al_2O_3 and Y_2O_3' and 'Silicon Yttrium Oxynitrides' by R. R. Wills," J. Amer. Ceram. Soc. 59 [1-2] 86 (1976).

11. C. Hamon, R. Marchand, M. Maunaye, J. Gaude and J. Guyader, "III. - Les Oxynitrures $Ln_{10}Si_6O_{24}N_2$ et quelqnes series analogues $(Ln, M)_{10}Si_6O_{24}X_2$ (X = N, O, F) Obtenues par Substitution," Rev. Chim. Min. 12, 259-67 (1975).

12. F. F. Lange, "Task I: Fabrication, Microstructure and Selected Properties of SiAlON Compositions," Final Report Naval Air Systems Command, Contract N00019-73-C-0208, Feb. 26, 1974.

13. L. J. Gauckler, H. L. Lukas, G. Petzow, "Contribution to the Phase Diagram Si_3N_4-AlN-Al_2O_3-SiO_2," J. Amer. Ceram. Soc. 58 [7] 346 (1975).

14. I. C. Huseby, H. L. Lukas, and G. Petzow, "Phase Equilibria in the System Si_3N_4-SiO_2-BeO-Be_3N_4," J. Amer. Ceram. Soc. 58 [9], 377 (1975).

15. J. W. Visser, "A Fully Automatic Program for Finding the Unit Cell from Powder Data," J. Appl. Cryst. 2, 89 (1969).

16. N. B. Pilling and R. E. Bedworth, "Oxidation of Metals at High Temperatures," J. Inst. Metals 29, 529 (1923).

17. N. A. Toropov and I. A. Bondar, "Phase Diagrams of the Binary Systems Sm_2O_3-SiO_2 and Yb_2O_3-SiO_2, and Comparison of These Silicates with the Other Rare Earth Element Silicates," Izvestiya Aked. Nank, Otdelemie Khimi. No. 8, 1372-79 (1961).

18. P. Kofstad, High Temperature Oxidation of Metals, John Witley, New York (1966).

FIGURE CAPTIONS

Figure 1 - Experimental phase relations in the Si_3N_4-SiO_2-Y_2O_3 system determined from specimens hot-pressed at temperatures between 1600° and 1750°C. Closed circles represent compositions examined.

Figure 2 - Weight gain due to oxidation at 1000°C for 20 hrs vs mole fraction of $Si_3Y_2O_3N_4$ in two phase Si_3N_4 bodies. (see Fig. 1 for compositions of a, b, c and d).

Figure 3 - An extreme example of the type of degradation that occurs for a polyphase body containing one of the four unstable phases oxidized at 1000°C. Specific example is composition d (see Fig. 1), oxidized for 20 hrs in air (original size: 0.3 x 0.6 3 cm).

Figure 4 - Weight change data for $Si_3Y_2O_3N_4$ oxidized at different temperatures in different atmospheres.

Figure 5 - a) Cross section (approx. size 0.3 x 0.6 cm) of a $Si_3Y_2O_3N_4$ specimen oxidized in air for 144 hrs at 1000°C showing thick oxide scale; b) SEM micrograph of oxide scale showing extensive cracking.

TABLE 1

CATION IMPURITIES (wt %) DETERMINED BY SPECTROGRAPHICAL ANALYSIS

Cation \ Powder	Si_3N_4	SiO_2	Y_2O_3
Al	0.052	0.03	< 0.005
Ag	< 0.001	< 0.001	--
B	< 0.01	< 0.003	--
Ca	0.011	< 0.005	< 0.005
Co	0.002	< 0.003	--
Cr	0.02	< 0.003	--
Fe	>0.10	0.012	< 0.001
Mg	0.003	0.001	< 0.005
Mn	0.024	< 0.001	< 0.005
Mo	0.002	< 0.001	--
Ni	0.014	< 0.001	--
Pb	< 0.01	< 0.01	--
Si	> 10	> 10	< 0.001
Ti	0.012	0.008	< 0.005
V	0.016	< 0.001	--
Zn	0.011	< 0.01	--
Zr	0.004	0.003	--

TABLE 2

OBSERVED X-RAY DIFFRACTION DATA FOR THE Y-Si-O-N COMPOUNDS

$Si_3Y_2O_3N_4$		$YSiO_2N$		$Y_{10}Si_7O_{23}N_4$		$Y_4Si_2O_7N_2$	
d(Å)	I/I_o	d(Å)	I/I_o	d(Å)	I/I_o	d(Å)	I/I_o
5.37	10	5.38	5			7.30	15
4.91	15						
				4.69	5		
		4.57	40			4.57	15
						4.35	10
		4.30	5				
				4.05	25		
				3.85	10		
3.63	25	3.60	5				
		3.52	100				
3.39	15						
				3.39	20		
		3.29	25				
						3.22	20
				3.13	40		
		3.07	20	3.07	45		
3.00	35	2.99	5			3.07	100
						2.93	15
		2.87	10			2.87	30
						2.84	50
2.80	100	2.80	85	2.80	100		
		2.78	65				
				2.74	55		
2.68	5	2.70	5	2.70	40		
				2.60	10		
						2.61	5
						2.53	15
						2.51	15
2.46	15	2.45	5				
2.40	25	2.40	5				
2.35	5						
2.33	5						
		2.28	23				
2.23	5					2.27	10
				2.25	10		
				2.21	5		
2.16	5						
				2.11	5		
		2.03	60	2.03	15	2.05	10
1.99	25			2.00	30	1.99	15

TABLE 3

OBSERVED AND CALCULATED DIFFRACTION DATA FOR $YSiO_2N$

(Å)	hkl	Relative Intensity	Q_{obs}	Q_{cal}
5.38	111	5	0.0345	0.0346
4.57	200	40	0.0479	0.0480
4.30	002	5	0.0541	0.0541
3.60	022	5	0.0772	0.0772
3.52	131	100	0.0807	0.0808
3.29	040	25	0.0924	0.0924
3.07	031(041)	20	0.1061	0.1060(0.1059)
2.99	$22\bar{2}(22\bar{2})$	5	0.1118	0.1119(0.1119)
2.87	003(141)	10	0.1214	0.1216(0.1213)
2.80	013	85	0.1276	0.1275
2.78	$11\bar{3}$	65	0.1294	0.1295
2.70	311	5	0.1372	0.1373
2.45	$123(15\bar{1})$	5	0.1666	0.1667(0.1666)
2.40	033(151)	5	0.1736	0.1736(0.1732)
2.28	$40\bar{1}(250)$	25	0.1924	0.1924(0.1924)
2.03	$42\bar{2}$	60	0.2427	0.2427
1.92	*	30	--	--
1.90	*	20	--	--
1.86	*	15	--	--

Monoclinic, a = 9.208 Å, b = 13.157 Å, c = 8.675 Å, β = 97.471 Å

*hkl were not determined

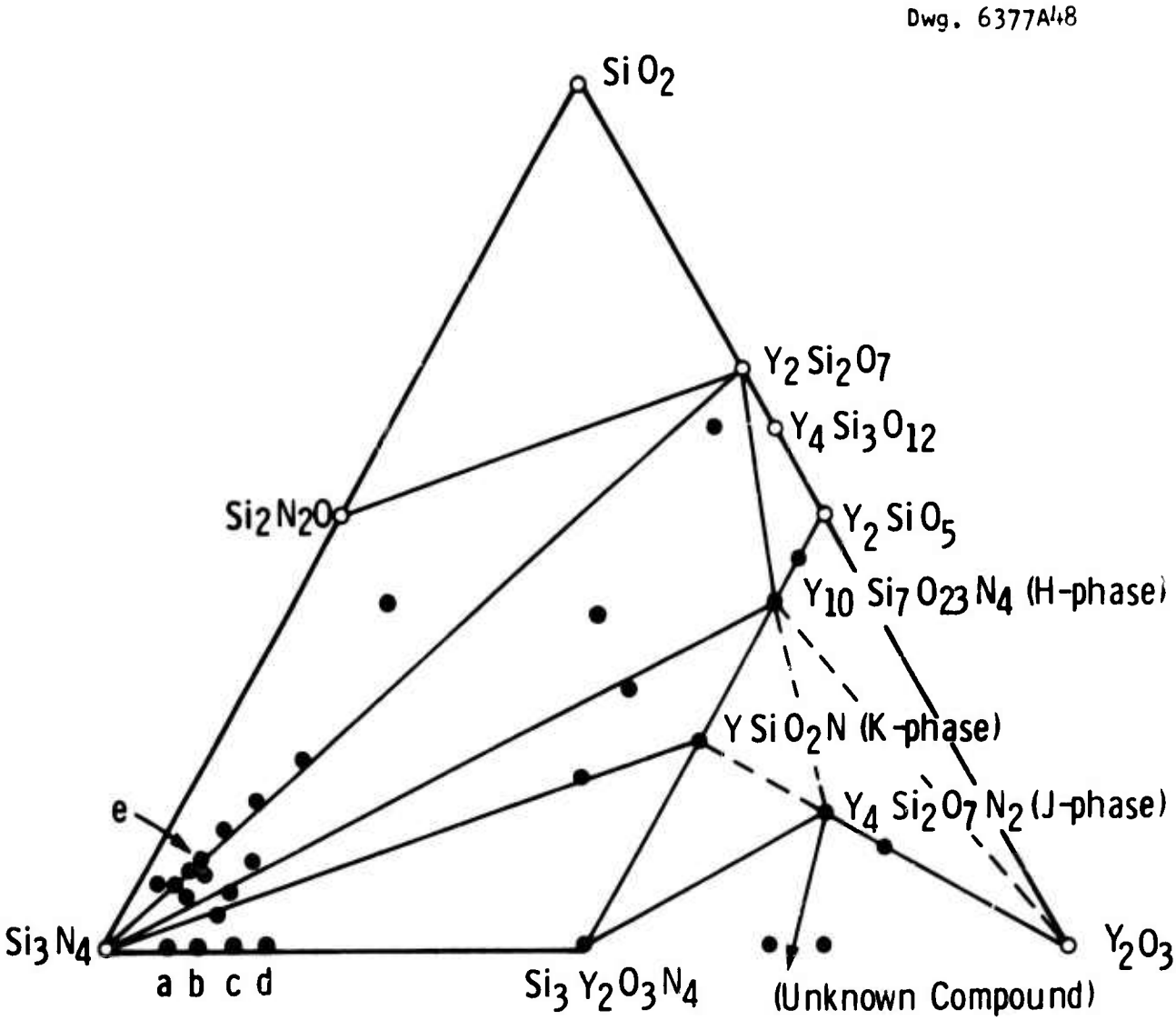

FIG. 1 -- Experimental phase relations in the Si_3N_4-SiO_2-Y_2O_3 system determined from specimens hot-pressed at temperatures between 1600° and 1750°C. Closed circles represent compositions examined.

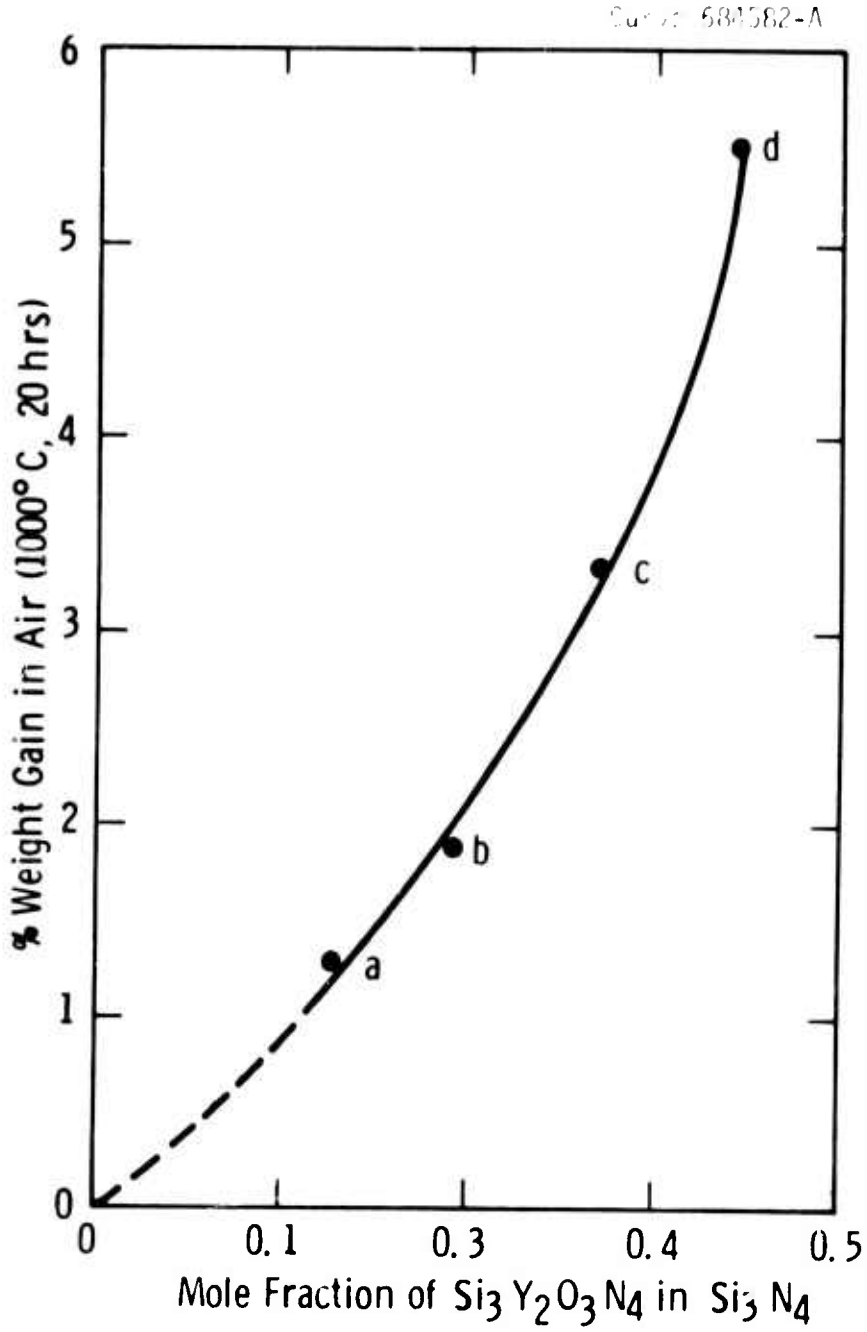

FIG. 2 -- Weight gain due to oxidation at 1000°C for 20 hrs vs mole fraction of $Si_3Y_2O_3N_4$ in two phase Si_3N_4 bodies. (see Fig. 1 for compositions of a, b, c and d).

FIG. 3 -- An extreme example of the type of degradation that occurs for a polyphase body containing one of the four unstable phases oxidized at 1000°C. Specific example is composition d (see Fig. 1), oxidized for 20 hrs in air (original size: 0.3 x 0.6 3 cm).

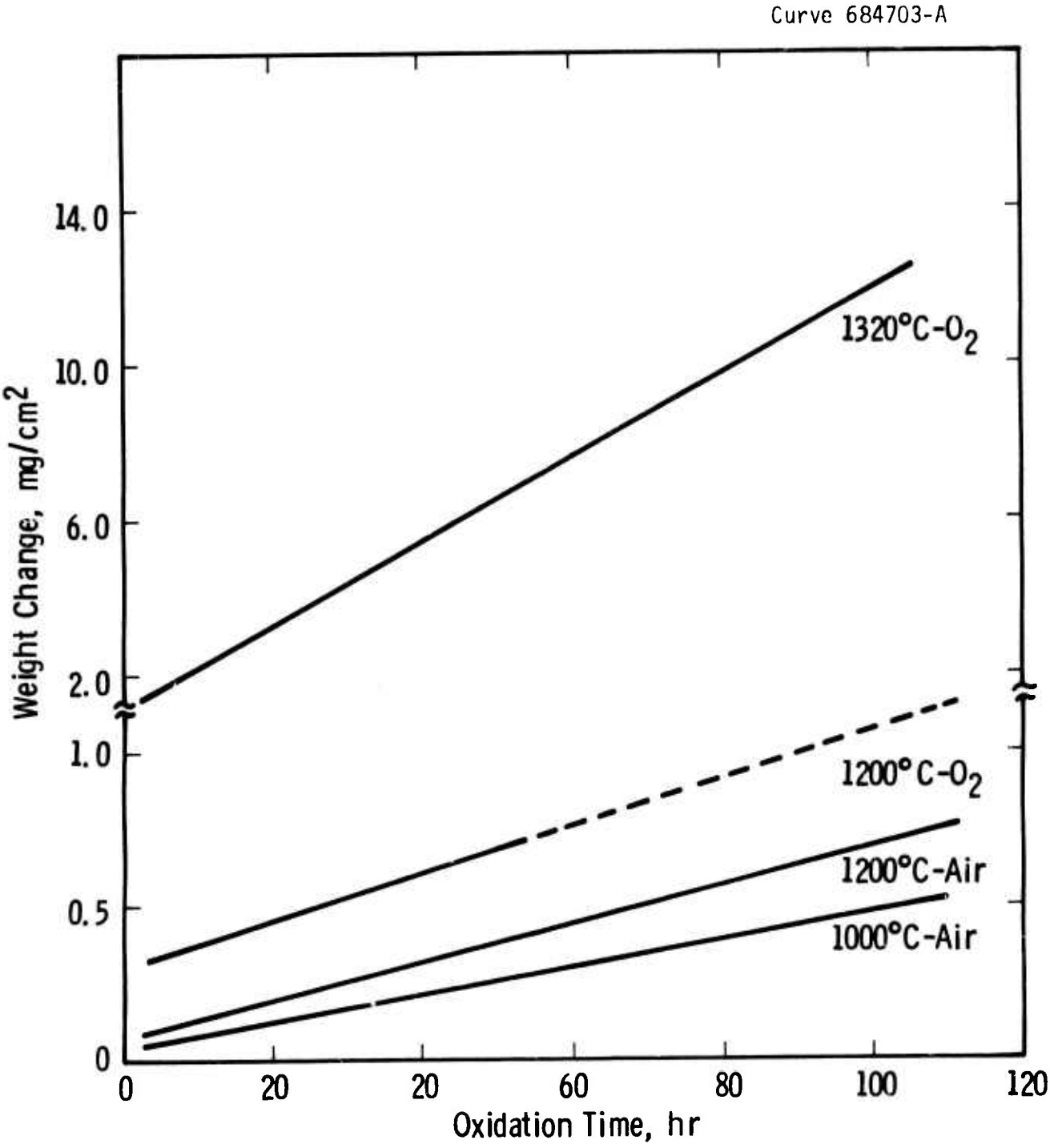

FIG. 4 -- Weight change data for $Si_3Y_2O_3N_4$ oxidized at different temperatures in different atmospheres.

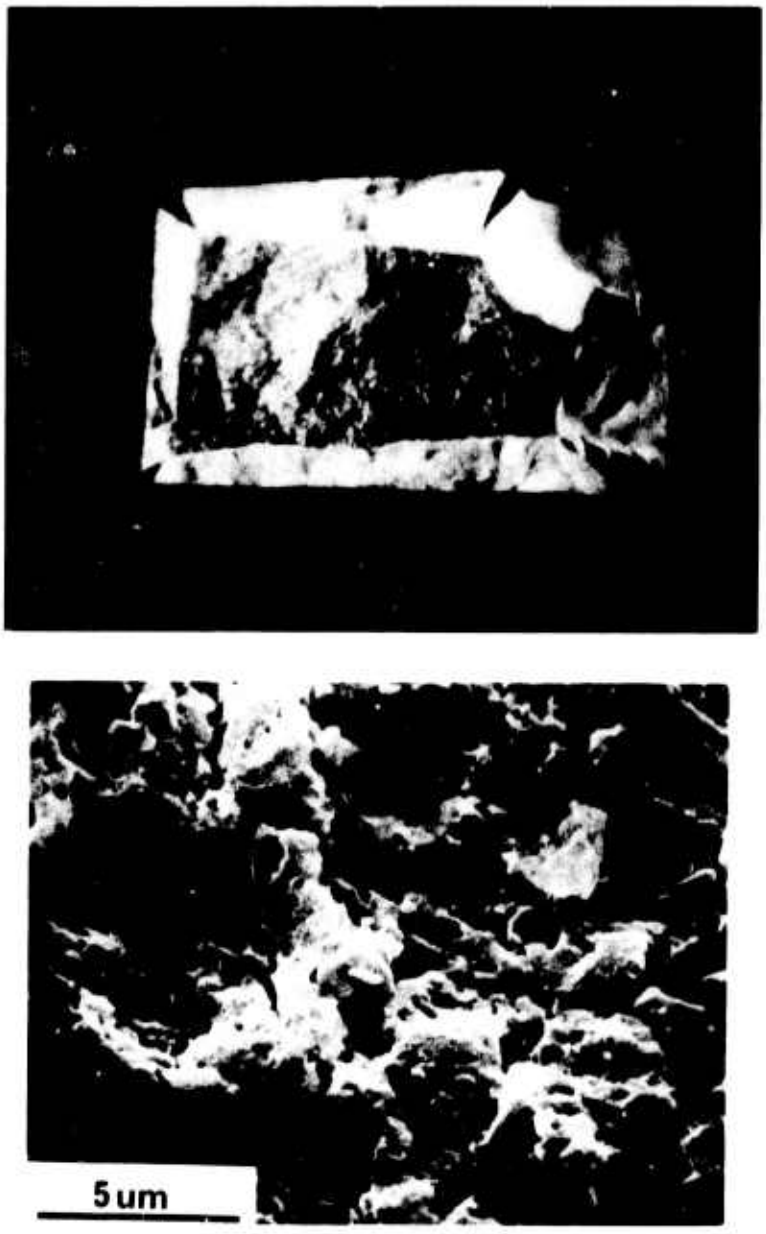

FIG. 5 -- a) Cross section (approx. size 0.3 x 0.6 cm) of a $Si_3Y_2O_3N_4$ specimen oxidized in air for 144 hrs at 1000°C showing thick oxide scale; b) SEM micrograph of oxide scale showing extensive cracking.

DEVELOPMENT OF MICROSTRUCTURE, STRENGTH AND FRACTURE TOUGHNESS OF HOT-PRESSED Si_3N_4

J. L. Iskoe and F. F. Lange

Technical Report #7, April 1, 1976

Westinghouse Electric Corporation
Research and Development Center

Contract Number N00014-74-C-0284

Sponsored by the Advanced Projects Agency
ARPA Order Number 2697
Program Code Number 01269

Scientific Officer: Dr. A. M. Diness
Office of Naval Research

Principal Investigator: Dr. F. F. Lange
(412) 256-3684

Effective Date of Contract: April 1, 1974

Contract Expiration Date: June 30, 1976

Amount of Contract: $159,892

Form Approved, Budget -- No. 22-R0293

Unclassified

SECURITY CLASSIFICATION OF THIS PAGE *(When Data Entered)*

REPORT DOCUMENTATION PAGE		READ INSTRUCTIONS BEFORE COMPLETING FORM
1. REPORT NUMBER	2. GOVT ACCESSION NO.	3. RECIPIENT'S CATALOG NUMBER
4. TITLE *(and Subtitle)* DEVELOPMENT OF MICROSTRUCTURE, STENGTH AND FRACTURE TOUGHNESS OF HOT-PRESSED Si_3N_4		5. TYPE OF REPORT & PERIOD COVEREO Technical Report #7 April 1, 1976 6. PERFORMING ORG. REPORT NUMBER
7. AUTHOR(s) J. L. Iskoe and F. F. Lange		8. CONTRACT OR GRANT NUMBER(s) N00014-74-C-0284
9. PERFORMING ORGANIZATION NAME ANO ADDRESS Westinghouse Research & Development Center Pittsburgh, Pennsylvania 15235		10. PROGRAM ELEMENT, PROJECT, TASK AREA & WORK UNIT NUMBERS
11. CONTROLLING OFFICE NAME AND ADDRESS		12. REPORT OATE April 1, 1976 13. NUMBER OF PAGES 18
14. MONITORING AGENCY NAME & ADDRESS*(if different from Controlling Office)*		15. SECURITY CLASS. *(of this report)* Unclassified 15a DECLASSIFICATION/OOWNGRAOING SCHEOULE

16. OISTRIBUTION STATEMENT *(of this Report)*

Reproduction in whole or in part is permitted for any purpose of the U.S. Government. Distribution of this document is UNLIMITED.

17. DISTRIBUTION STATEMENT *(of the abstract entered in Block 20, if different from Report)*

18. SUPPLEMENTARY NOTES

19. KEY WOROS *(Continue on reverse side if necessary and identify by block number)*

silicon nitride, hot, microstructure, strength, fracture, pressing, toughness

20. ABSTRACT *(Continue on reverse side if necessary and identify by block number)*

The microstructural development of silicon nitride, hot-pressed from ahigh α-phase powder with MgO additions, was observed with the aid of the SEM. The extent of the concurrent processes of densification, α→β phase transformation, and development of mechanical properties was determined as a function of time, temperature and MgO content. Full densification occurred

DD FORM 1 JAN 73 1473 EOITION OF 1 NOV 65 IS OBSOLETE

A-11

Unclassified

SECURITY CLASSIFICATION OF THIS PAGE *(When Data Entered)*

20. (Cont'd)

prior to the completion of the $\alpha \rightarrow \beta$ phase transformation. Maximum strength was virtually independent of hot-pressing time and temperature, once full density was achieved. A model which assumes that pre-existing β-grains are the nucleating grain growth sites for the transformed β-Si_3N_4 suggests that the aspect ratio (R) of the fiberous grains is independent of the original particle size and depends only on the initial α/β ratio, $R = 1 + \alpha/\beta$.

ABSTRACT

The microstructural development of silicon nitride, hot-pressed from a high α-phase powder with MgO additions, was observed with the aid of the SEM. The extent of the concurrent processes of densification, α→β phase transformation, and development of mechanical properties was determined as a function of time, temperature and MgO content. Full densification occurred prior to the completion of the α→β phase transformation. Maximum strength was virtually independent of hot-pressing time and temperature, once full density was achieved. A model which assumes that pre-existing β-grains are the nucleating grain growth sites for the transformed β-Si_3N_4 suggests that the aspect ratio (R) of the fiberous grains is independent of the original particle size and depends only on the initial α/β ratio, $R = 1 + \alpha/\beta$.

1. INTRODUCTION

Silicon nitride powder is hot-pressed to near theoretical density by incorporating small alloying additions prior to hot-pressing. The most commonly used hot-pressing aid is MgO. The MgO and the SiO_2 surface layer on each Si_3N_4 particle are believed to react at high temperatures to form a liquid[1] which causes the Si_3N_4 powder to consolidate by a solution-reprecipitation mechanism.[2,3]

Silicon nitride exists as two distinct crystallographic phases, viz., α and β. Although the relation between these two phases is still in question,* a previous investigation[4,5] has shown that stronger and tougher material can be fabricated with predominantly α-phase powder. This is probably due to the fiberous grain structure of the material hot-pressed from α-Si_3N_4 powder in contrast with the equiaxed grain morphology resulting from a β phase powder.[4,5]

*Overwhelming evidence[6-10] indicates the proposed hypothesis that oxygen stabilizes[11] α-Si_3N_4 is incorrect.

The present work was primarily undertaken to determine the conditions controlling the development of the fiberous grain morphology of Si_3N_4 hot-pressed with α-phase powder and to concurrently observe the development of mechanical properties.

2. EXPERIMENTAL

2.1 Powder Preparation and Fabrication

Two blended batches of relatively pure, high α-phase Si_3N_4 powder (approximately 90% α, 10% β) produced at the Westinghouse Research Laboratory with only 160 ppm Ca, no detectable alkaline elements and 1.6 wt % oxygen* (6.7 mole % SiO_2) was used for this study.** Table 1 lists the impurities as determined by spectrographic analysis.

Powder batches of ∿ 100 g were prepared for fabrication by adding 5 wt % (15 mole %) of a high purity MgO*** and milling for 16 hours in plastic bottles using WC media and t-butanol. After drying and breaking up agglomerates, 5 cm diameter by 1 cm thick discs were hot-pressed at 28 MN/m^2 in a Grafoil**** lined graphite die in a N_2 atmosphere at temperatures between 1600°C and 1800°C for periods between 30 seconds to 4 hours. A heating rate of ∿ 35°C/min was maintained between 25°C and 1600°C. Density was determined by the Archimedes technique.

2.2 Microstructural Observations

A fracture surface from each disc was etched in concentrated (48%) HF for 48 hours, to dissolve the silicate grain boundary phase

---

* Determined by an inert gas fusion, thermoconductivity method.

** High purity powder was used to minimize the degradation of high temperature mechanical properties as reported elsewhere.(5)

*** < 20 ppm total cation impurity as determined by spectrographic analysis. United Mineral and Chemical Corp., NY, NY.

**** Trade Mark, Union Carbide Corporation.

exposing the morphology of the Si_3N_4 grains.* At least three areas of each specimen were observed in a SEM by randomly zooming into each area to a magnification of 5000X. When a fiberous microstructure was encountered, only qualitative observations could be made due to the uncertainty of the aspect ratio of each grain.

The phase content of each material was determined by X-ray diffraction analysis.

2.3 Strength and Fracture Toughness

Three, 4-pt flexural strength determinations were made at 25°C and 1400°C in air for materials with densities > 95% of theoretical. The bar specimens were cut, ground and tested as described previously.(5)

The critical stress intensity factor, K_c, was determined using double-beam-cantilever specimens cut from 2 cm thick billets hot-pressed under conditions to achieve both full density and different α/β ratios. The normal of the crack plane in these specimens was parallel to the hot-pressing direction. Specimen preparation, dimensions and testing are the same as described previously.(4)

3. RESULTS

3.1 Densification and $\alpha \rightarrow \beta$ Transformation

The percent theoretical density and β-Si_3N_4 content are presented in Fig. 1 as a function of time and temperature for Si_3N_4 hot-pressed with 5 w/o MgO. Densification was a more rapid process than the $\alpha \rightarrow \beta$ transformation, i.e., at all temperatures, densification was

*It is impossible to fully expose randomly oriented fiberous and/or plate-like grain morphologies by sectioning, polishing and etching due to the high probability of intercepting the fiber axis and/or the plate axis at random with the sectioning plane. That is, relatively few fibers and/or plates will lie in the sectioning plane.

complete before the phase transformation. This result was also obtained by Weston and Carruthers.[3] The phase transformation was also shown to be more sensitive to temperature changes than the densification process.

Figure 2 illustrates that, at a given temperature, both the densification and transformation rates decrease with smaller additions of MgO. But, again, densification is the more rapid process.

3.2 Development of Grain Structure

Figure 3 is a representative micrograph of a material (54% dense, 15% β-phase) hot-pressed at 1600°C for 30 seconds, illustrating that the majority of the α-Si_3N_4 particles are equiaxed in shape with sizes ranging from ∿5 μm to < 0.1 μm. This observation strongly suggests that the milled powder had a similar morphology and size distribution.*

Microstructural observations of materials hot-pressed for periods between 0.5 to 120 minutes at 1700°C, 1750°C and 1800°C showed that a fiberous morphology developed from equiaxed grains. Qualitative observations**, illustrated with representative micrographs in Figs. 4 and 5, indicated that the fiberous grain content was proportional to the β-phase content and not to the density, suggesting that the development of the fiberous grain morphology was simultaneous with the α to β transformation. Materials with a β-phase content of 100% contained few, if any, equiaxed grains; the microstructure of such materials consisted of densely packed small and large 'diameter' fibers. No significant difference in grain size or morphology could be observed between the fully transformed materials hot-pressed at different temperatures and times.

---

* An analysis with a Micromeritics Particle Size Analyzer indicates an average particle size of 2 μm, with sizes ranging from 10 μm to < 0.5 μm. White[12] has used a SEM technique to analyze the morphology of similar milled Si_3N_4 powders, showing that the aspect ratio of the particles is ∿ 1.

** Due to the random orientations of the fiber-like (transformed) β-Si_3N_4 grains, it was impossible to unambiguously determine their length, aspect ratio and volume content. It was difficult to differentiate fiberous and equiaxed grains for β contents ≤ 40%.

3.3 Strength and Fracture Toughness

The flexural strength at 25°C and 1400°C of all materials with a density $\geq$ 95%* of theoretical is shown in Fig. 6 as a function of the transformed β-phase content. Each point, represented by a symbol indicating a hot-pressing temperature between 1650°C and 1800°C, is an average value for one material. Circled points represent materials with densities between 95% and 97% of theoretical.

The room temperature strengths exhibited significantly more scatter, both within a single material (not shown in Fig. 6) and between the different materials, than exhibited by strengths at 1400°C. This difference in strength variation is due to the sub-critical crack growth that occurs in hot-pressed Si_3N_4 at elevated temperatures, which reduces the large dependency of strength on the initial distribution of crack sizes.[13] If only the materials hot-pressed between 1700°C and 1800°C with α-phase powder to densities > 98% are considered, strengths at both temperatures appear to be independent of hot-pressing temperature, period and β-phase content. If the somewhat lower density materials (between 95% and 98% of theoretical) and material hot-pressed at 1650°C are included, some strength reduction appears at β-phase contents < 50%.

The critical stress intensity factor for four fully dense materials, including a material fabricated for a previous investigation with a high β-phase powder (∿ 90% β, ∿10% α), is shown in Fig. 7 as a function of the β-phase content. Although the average values increase by 20% from 4.65 $MN/m^{3/2}$ to 5.50 $MN/m^{3/2}$) for β-phase contents of 40% to 100%, respectively, the large scatter in data for the 40% β-phase material precludes a strong relation between fracture toughness and β-phase content.

---

*Plotting strengths of materials with densities < 95%, which were generally materials with β-Si_3N_4 contents < 40%, could be erroneous due to the effect of porosity on the elastic modulus and thus strength.

4. DISCUSSION

4.1 Development of Microstructure

A principal result of this investigation is that the growth of the fiberous β-Si_3N_4 grains is shown to be related to the α-β phase transformation. The model that is most consistent with this relation and other observations is the solution of the α-Si_3N_4 grains in the liquid present at the hot-pressing temperature and the subsequent precipitation of β-Si_3N_4.* Since the liquid is present both during and after densification as indicated by densification studies[2] and other microstructural observations,[14,15] the solution of α-Si_3N_4 and precipitation of β-Si_3N_4 would occur both during and after densification. Full densification only requires a portion of the initial powder (30-40%) to dissolve and precipitate, therefore, much of the α→β transformation should take place after densification is complete.

The preferred precipitation sites would be pre-existing β-Si_3N_4 grains, which would cause their preferred, fiberous growth and their eventual consumption of the α-Si_3N_4 grains at the conclusion of the α→β transformation. Once the principal thermodynamic driving force, i.e., the α→β transformation**, for grain growth is no longer present, the grain structure becomes relatively stable as indicated by the similar microstructure of 100% β-phase materials hot-pressed with α-phase powder for different temperatures and time periods.

The above model indicates that the number of fiberous β-grains (or nucleating sites) in a fully transformed material will correspond to the number of β-Si_3N_4 particles in the initial powder. If it is assumed that the grain growth perpendicular to the fiber axis is negligible, two important consequences of the model can be hypothesized. First, the

---

*The solution-precipitation of β-Si_3N_4 is also expected; but it is implied here that the solution of α-Si_3N_4 and precipitation of β-Si_3N_4 is the preferential reaction.

**It is assumed that the α and β structures are, respectively, low and high temperature polymorphs of Si_3N_4.

aspect ratio (R) of the fiberous β-Si_3N_4 grains will be proportional to the α/β ratio as given by

$$R = 1 + \frac{\alpha}{\beta} .$$

This equation is obtained by letting the diameter of the β-Si_3N_4 grain tc remain constant and its length parallel to the c axis (fiber axis) increase in proportion to the consumed α-Si_3N_4. This relation predicts that the aspect ratio for powders used in the present investigation should be 7-10, and an aspect ratio of $\sim$ 1 for materials hot-pressed with a high β-phase powders. Second, the distribution of fiber diameters will be related to the distribution of β-Si_3N_4 particle sizes in the initial powder. These ideas may be important in controlling the microstructure of hot-pressed Si_3N_4.

4.2 Development of Strength and Fracture Toughness

A previous investigation[4] showed that material fabricated with high α-Si_3N_4 powder is twice as strong and has twice the fracture toughness as material fabricated with β-Si_3N_4 powder. This difference in fracture toughness and strength was attributed to the fiberous grain structure of material fabricated with α-Si_3N_4 powder relative to the equiaxed grain structure produced from β-Si_3N_4 powder.

The current investigation has neither substantiated nor disproved this hypothesis. Coe, et al.,[16] have reported a much stronger dependence of strength on the β phase content. For the data reported here some decrease in strength and fracture toughness with decreasing β content could be interpreted, but the scatter in data precludes any strong relation. Further work is therefore required to test the original hypothesis.

ACKNOWLEDGMENTS

The authors wish to thank W. J. Carmen and J. J. Nalevanko for their technical assistance and R. C. Kuznicki for the X-ray diffraction analysis. This work was supported by the Advanced Research Projects Agency and monitored by the Office of Naval Research under Contract No. N00014-74-C-0284.

REFERENCES

1. S. Wild, P. Grieveson, K. H. Jack and M. J. Latimer, "Role of Magnesia in Hot-Pressed Si_3N_4", Special Ceramics 5, Ed. by P. Popper, pp. 377-384, BCRA, Stoke-on-Trent, England, 1972.

2. G. R. Terwilliger and F. F. Lange, "Hot-Pressing Behavior of Si_3N_4", J. Am. Ceram. Soc. 57, [1], 25-29 (1974).

3. R. J. Weston and T. G. Carruthers, "Kinetics of Hot-Pressing of α-Si_3N_4 Powder with Additives", Proc. Brit. Ceram. Soc. No. 22, 197-206 (1973).

4. F. F. Lange, "Relation Between Strength, Fracture Energy and Microstructure of Hot-Pressed Si_3N_4", J. Am. Ceram. Soc. 56, [10] (1973).

5. J. L. Iskoe, F. F. Lange and E. S. Diaz, "Effect of Selected Impurities on the High Temperature Mechanical Properties of Hot-Pressed Si_3N_4", J. Mat. Sci. (in press).

6. H. F. Priest, F. C. Burns, G. L. Priest and E. C. Skaar, "Oxygen Content of α-Si_3N_4", J. Am. Ceram. Soc. 56, [7], 395 (1973).

7. A. J. Edwards, D. P. Elias, M. W. Lindley, A. Atkinson, A. J. Moulson, "Oxygen Content of Reaction Bonded α-Si_3N_4", J. Mat. Sci. 9, 516 (1974).

8. F. F. Lange, "Task I: Fabrication, Microstructure and Selected Properties of SiAlON Compositions", Final Rept. Contract No. N00019-73-C-0208, Naval Air Systems Command, Feb. 26, 1974.

9. I. Kohatsu and J. W. McCauley, "Re-Examination of the Crystal Structure of α-Si_3N_4", Mat. Res. Bull. 9, 917 (1974).

10. Katsuo Kato, Zenzaburo Inoue, Kazunovi Kijima, Isao Kawada, Hirokichi Tanaka and Tsuneko Yamane, "Structural Approach to the Problem of Oxygen Content in α-Si_3N_4", J. Am. Ceram. Soc. 58, [3-4], 90-91, (1975).

11. S. Wild, P. Grieveson and K. H. Jack, "Crystal Structures of α and β-Si_3N_4 and Ge_3N_4, Special Ceramics 5, Ed. by P. Popper, p. 385, B.C.R.A., Stoke-on-Trent, (1974).

12. E. W. White, The Pennsylvania State University, private communication.

13. R. J. Charles, "Dynamic Fatigue of Glass", J. Appl. Phys. 29, [12], 1657 (1958).

14. A. G. Evans and J. V. Sharp, "Microstructural Studies on Si_3N_4", J. Mat. Sci. 6, [10], 1292-1302 (1971).

15. P. Drew and M. H. Lewis, "Microstructures of Si_3N_4 Ceramics During Hot-Pressing Transformations", J. Mat. Sci. 9, 261-269 (1974).

16. R. F. Coe, R. J. Lumby and M. F. Pawson, "Some Properties and Applications of Hot-Pressed Si_3N_4", Special Ceramics 5, Ed. by P. Popper, p. 361, B.C.R.A., Stoke-on-Trent (1974).

TABLE 1

Spectrographic Analyses of Westinghouse Si_3N_4 Starting Powder (wt %)

Al	0.08
Ag	< 0.001
B	0.001
Ca	0.016
Cr	0.01
Fe	> 0.1
Mg	0.001
Mn	0.05
Mo	< 0.003
Ni	< 0.01
Pb	< 0.01
Sb	< 0.01
Sn	< 0.01
Ti	0.01
V	0.005
Zn	< 0.01

FIGURE CAPTIONS

FIG. 1 -- Densification and α→β transformation as a function of hot-pressing temperature and time for Si_3N_4 densified with 5 w/o MgO.

FIG. 2 -- Densification and α→β transformation vs time for Si_3N_4 hot-pressed at 1750°C with either 2 w/o or 5 w/o MgO.

FIG. 3 -- Micrograph of etched fracture surface of Si_3N_4 (+ 5 w/o MgO) hot-pressed at 1600°C for 30 seconds (54% dense, 15% β content).

FIG. 4 -- Micrographs of etched fracture surfaces of Si_3N_4 (+ 5 w/o MgO) hot-pressed at 1700°C for different periods (% density and % β content are shown on micrographs).

FIG. 5 -- Micrographs of etched fracture surfaces of Si_3N_4 (+ 5 w/o MgO) hot-pressed at 1750°C for different periods (% density and % β content are shown on micrographs).

FIG. 6 -- Flexural strength vs β content for Si_3N_4 (+ 5 w/o MgO) with densities $\geq$ 95% of theoretical. Hot-pressing temperatures: x = 1650°C, ▲ = 1700°C, ● = 1750°C, ■ = 1800°C; circled points: density between 95-97% theoretical.

FIG. 7 -- Critical stress intensity factor vs β content for hot-pressed Si_3N_4 - see Fig. 6 for symbols.

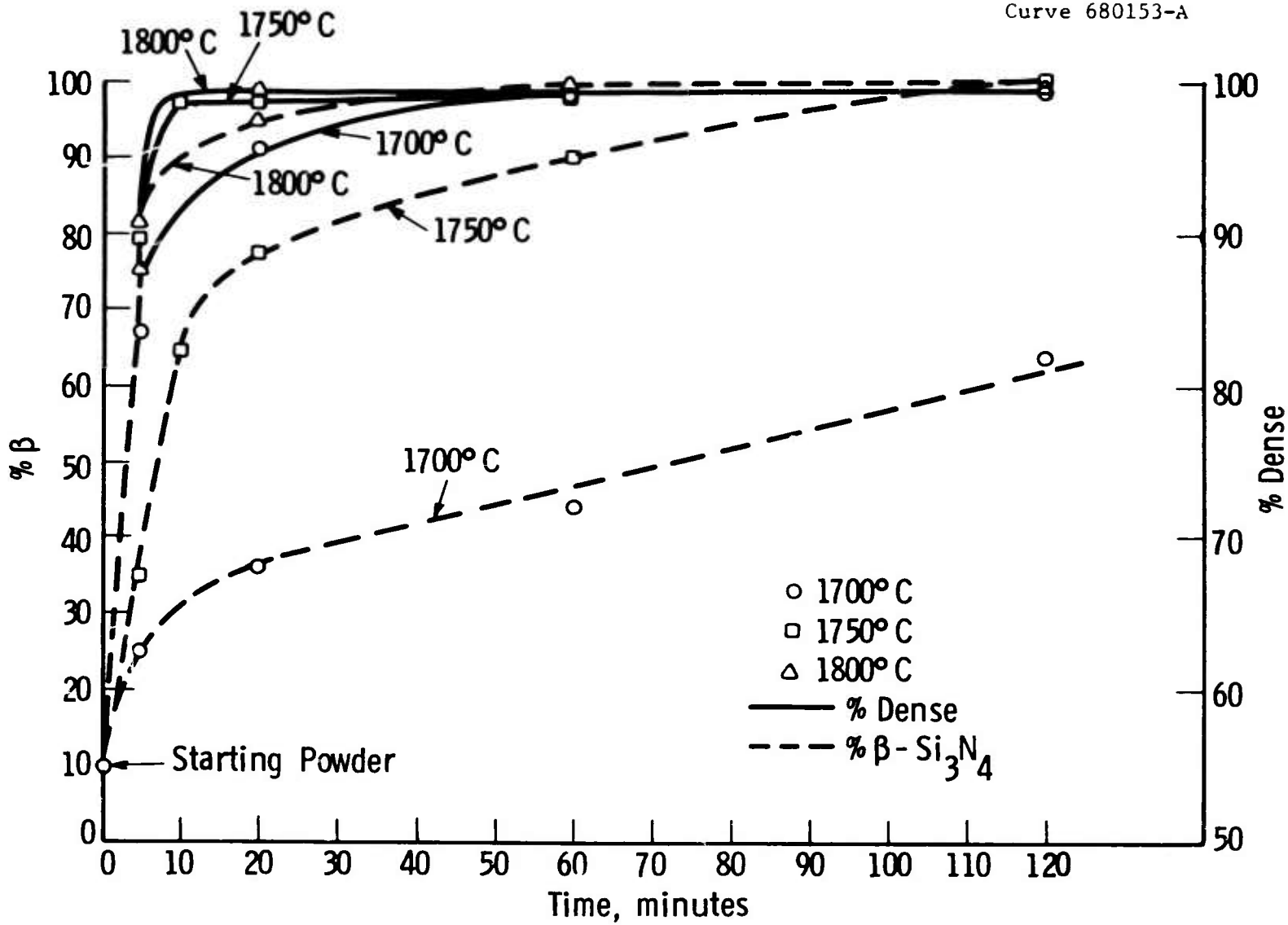

Fig. 1 — Densification and a→β transformation as a function of hot-pressing temperature and time for Si_3N_4 densified with 5 W/o MgO

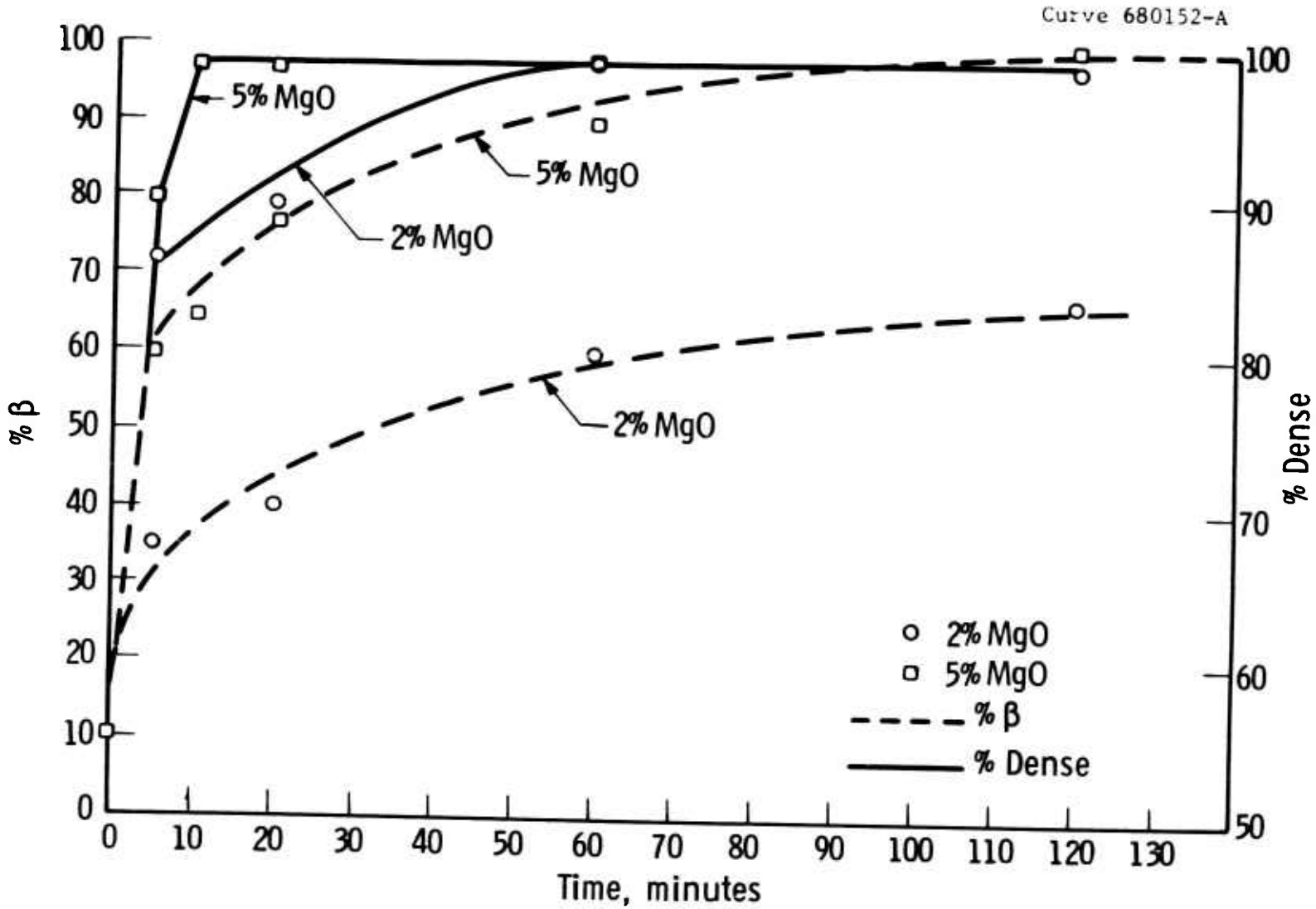

Fig. 2 — Densification and a→β transformation vs time for Si_3N_4 hot-pressed at 1750 °C with either 2 W/o or 5 W/o MgO

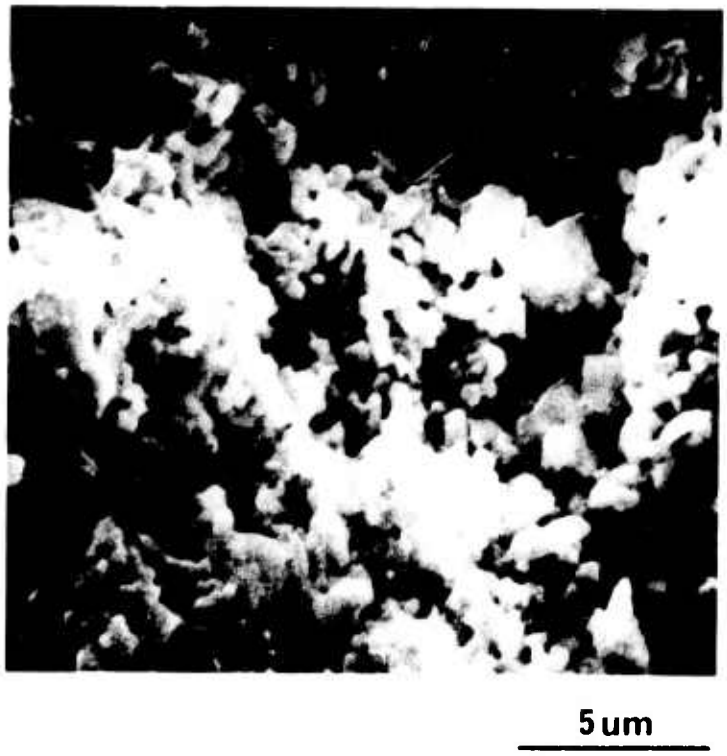

FIG. 3 -- Micrograph of etched fracture surface of Si_3N_4 (+ 5 w/o MgO) hot-pressed at 1600°C for 30 seconds (54% dense, 15% β content).

5 MINUTES ρ = 83.5% 25% β

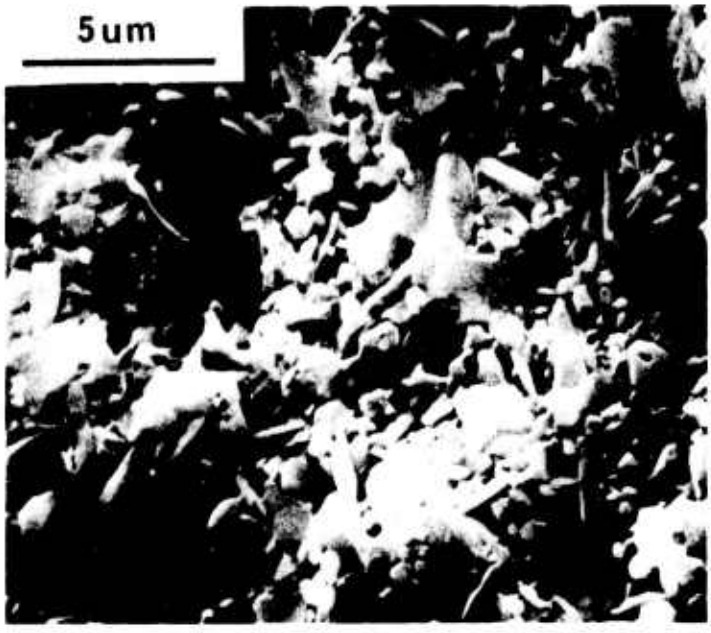

120 MINUTES ρ = 99.3 65% β

FIG. 4 -- Micrographs of etched fracture surfaces of Si_3N_4 (+ 5 w/o MgO) hot-pressed at 1700°C for different periods (% density and % β content are shown on micrographs).

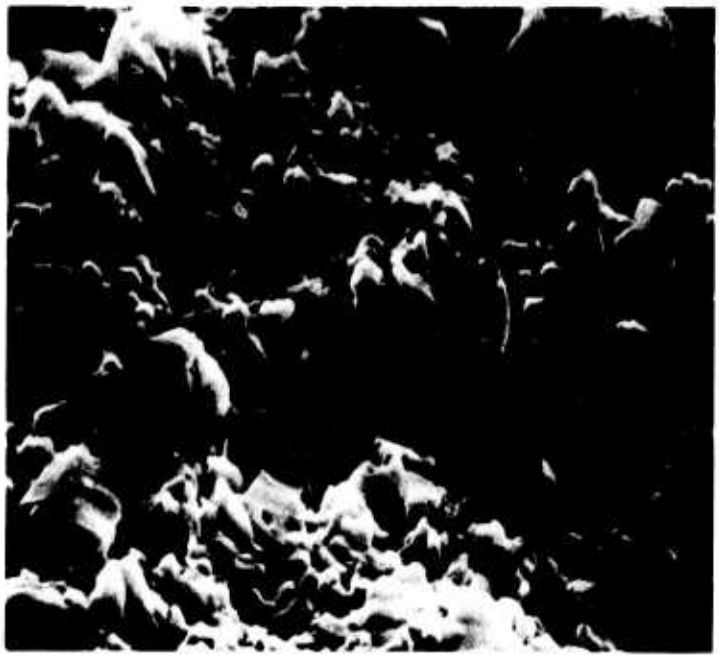

5 MINUTES ρ = 89.7% 35% β

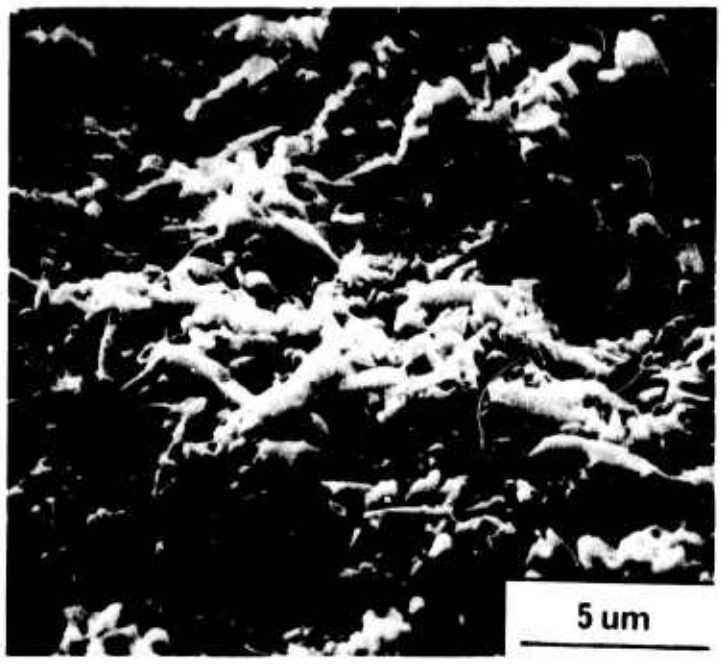

60 MINUTES ρ = 99.0% 90% β

FIG. 5 -- Micrographs of etched fracture surfaces of Si_3N_4 (+ 5 w/o MgO) hot-pressed at 1750°C for different periods (% density and % β content are shown on micrographs).

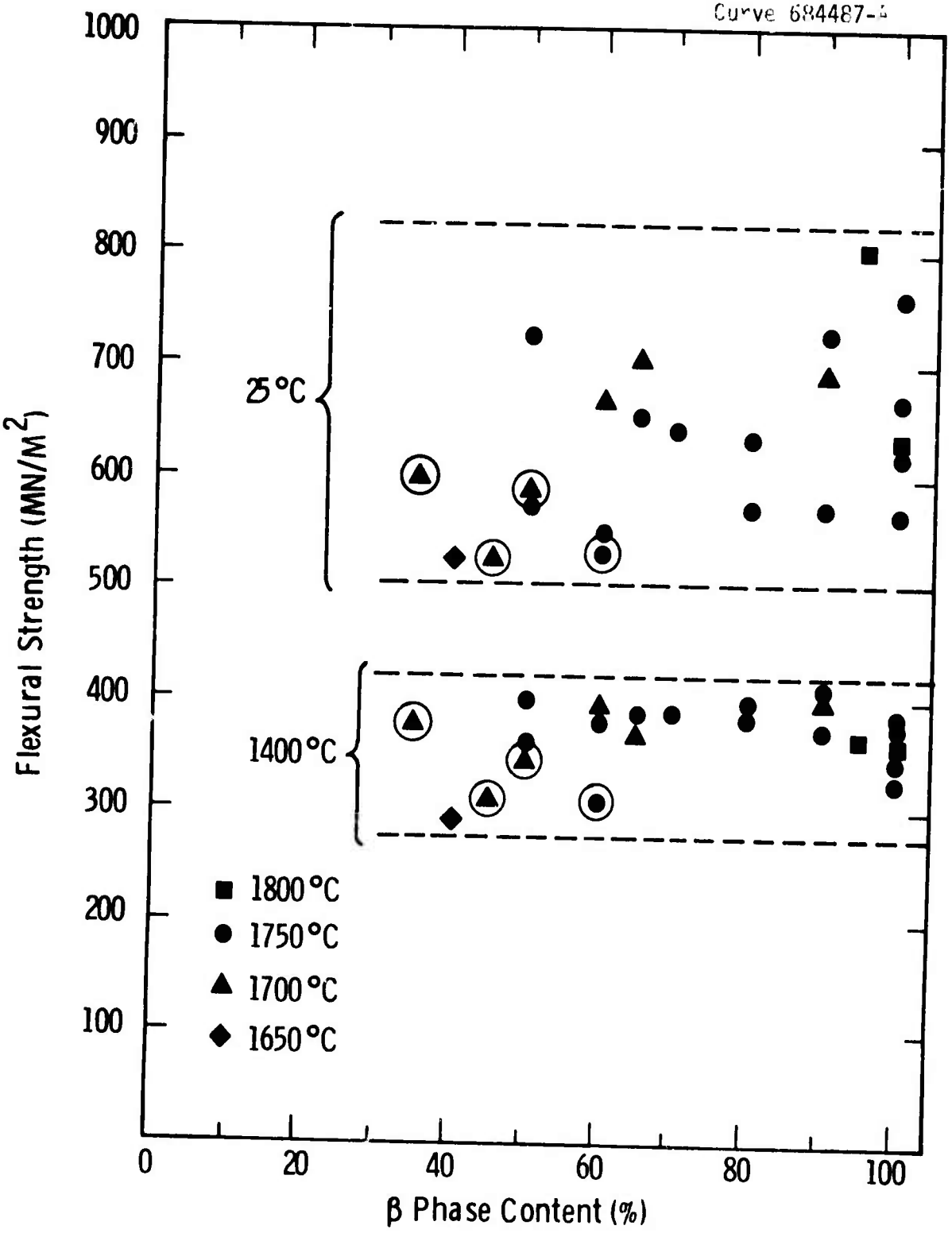

Fig. 6 — Flexural strength vs β content for Si_3N_4 (+ 5 W/o MgO) with densities ≥ 95% of theoretical. Hot-pressing temperatures: ◆ = 1650°C, ▲ = 1700°C, ● = 1750°C, ■ = 1800°C; circle points: density between 95 - 97% theoretical

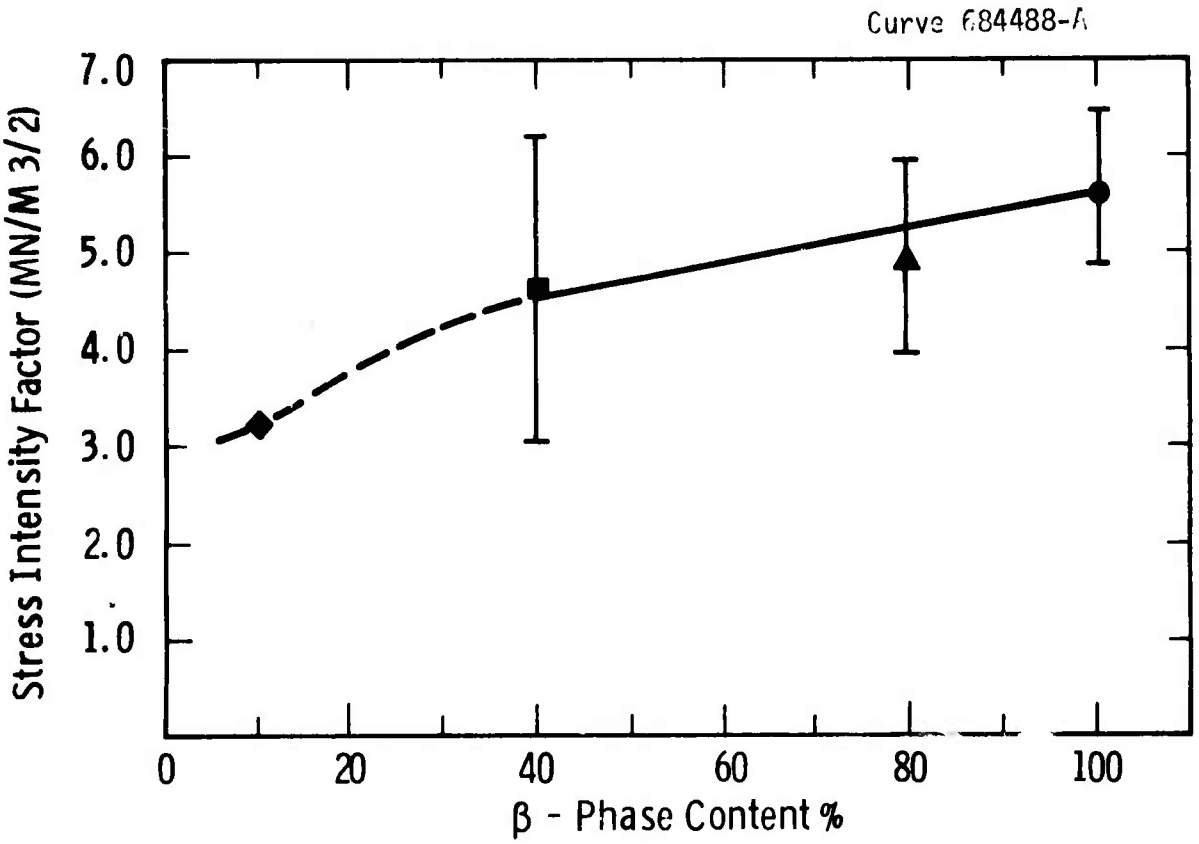

Fig. 7 – Critical stress intensity factor vs β content for hot-pressed Si_3N_4 - see Fig. 6 for symbols

SINTERING OF SiC WITH BORON COMPOUNDS

F. F. Lange and T. K. Gupta

Technical Report #8, April 1, 1976

Westinghouse Electric Corporation
Research and Development Center

Contract Number N00014-74-C-0284

Sponsored by the Advanced Projects Agency
ARPA Order Number 2697
Program Code Number 01269

Scientific Officer: Dr. A. M. Diness
Office of Naval Research

Principal Investigator: Dr. F. F. Lange
(412) 256-3684

Effective Date of Contract: April 1, 1974

Contract Expiration Date: June 30, 1976

Amount of Contract: $159,892

Form Approved, Budget -- No. 22-R0293

Unclassified

SECURITY CLASSIFICATION OF THIS PAGE (When Data Entered)

REPORT DOCUMENTATION PAGE		READ INSTRUCTIONS BEFORE COMPLETING FORM
1. REPORT NUMBER	2. GOVT ACCESSION NO.	3. RECIPIENT'S CATALOG NUMBER
4. TITLE (and Subtitle) SINTERING OF SiC WITH BORON COMPOUNDS		5. TYPE OF REPORT & PERIOD COVERED Technical Report #8 April 1, 1976 6. PERFORMING ORG. REPORT NUMBER
7. AUTHOR(s) F. F. Lange and T. K. Gupta		8. CONTRACT OR GRANT NUMBER(s) N00014-74-C-0284
9. PERFORMING ORGANIZATION NAME AND ADDRESS Westinghouse Research and Development Center Pittsburgh, Pennsylvania 15235		10. PROGRAM ELEMENT, PROJECT, TASK AREA & WORK UNIT NUMBERS
11. CONTROLLING OFFICE NAME AND ADDRESS		12. REPORT DATE April 1, 1976 13. NUMBER OF PAGES 14
14. MONITORING AGENCY NAME & ADDRESS(if different from Controlling Office)		15. SECURITY CLASS. (of this report) Unclassified 15a. DECLASSIFICATION/DOWNGRADING SCHEDULE

16. DISTRIBUTION STATEMENT (of this Report)

Reproduction in whole or in part is permitted for any purpose of the U.S. Government. Distribution of this document is UNLIMITED.

17. DISTRIBUTION STATEMENT (of the abstract entered in Block 20, if different from Report)

18. SUPPLEMENTARY NOTES

19. KEY WORDS (Continue on reverse side if necessary and identify by block number)

silicon carbide, sintering, boron, compounds

20. ABSTRACT (Continue on reverse side if necessary and identify by block number)

SiC powder was sintered with different amounts of either B + 1 w/o C or B_4C. Microstructural observations showed the presence of a B-rich second phase which may have been a liquid at the sintering temperatures suggesting a liquid phase sintering mechanism.

B-ii

DD FORM 1 JAN 73 1473 EDITION OF 1 NOV 65 IS OBSOLETE

Unclassified

SECURITY CLASSIFICATION OF THIS PAGE (When Data Entered)

SINTERING OF SiC WITH BORON COMPOUNDS

by

F. F. Lange and T. K. Gupta

Westinghouse Research Laboratories
Pittsburgh, Pennsylvania 15235

Prochazka's discovery[1] that submicron SiC powder could be sintered with the aid of B compounds lead to the experiments and observations reported by the present workers.

Cylindrical specimens (0.27 cm dia by 1.0 cm) were cold-pressed from powder mixtures containing β-SiC* and different amounts of either B + 1 w/o C or B_4C. Sintering experiments were performed in a tungsten element furnace containing 40-80 Torr of Ar, with the specimens supported on a graphite pedestal. The furnace temperature was recorded with a Pt-Re thermocouple placed close to the specimen. Furnace temperatures were in agreement with specimen temperatures which were measured through a vertical view port with an optical pyrometer. Weight and dimension measurements were used to determine density both before and after sintering. Representative specimens were sectioned for examination with light and electron optical tools.

All specimens lost weight at temperatures > 1900°C as illustrated in Fig. 1a for the case of β-SiC + 1 w/o B + 1 w/o C specimens

*PPG Industries, Pittsburgh, Pa.; surface area: 16 m^2/g, impurities reported elsewhere.(2)

sintered for 30 min. The surface of each specimen sintered above 1900°C was coated with a layer of carbon which could be removed by buffing. The thickness of the carbon layer appeared to increase with increasing temperature and/or sintering period. The decomposition of SiC at high temperatures is a well-known phenomenon[3] and it could account for the observed weight losses.*

The densities of the various specimens sintered between 1800°C and 2050°C for 30 min are shown in Fig. 1b. No significant difference was observed for powder compositions containing either 1 w/o B + 1 w/o C or 3 w/o B + 1 w/o C, both resulting in substantial densification. Experiments with additions of either 1 w/o B + 1 w/o C or 2 w/o B_4C at 2020°C for periods between 10 to 60 min resulted in similar densities ($\pm$2%) showing that densification at this temperature is very rapid. As shown in Fig. 1b, larger additions of B did not promote densification.

The geometrically determined densities reported in Fig. 1b include the C surface coating. Water immersion density determinations after the C coating was removed resulted in slightly higher (2-5%) densities.

The grain structure of dense specimens sintered at $\leq$ 2000°C consisted of larger, thin plate-like grains (~100 μm dia., < 3 μm thick) within an equiaxial, small ($\leq$ 2 μm) grain size matrix. At temperatures > 2000°C, a large proposition of the dense specimens contained only large (>100 μm), thick plate-like grains. Previous investigations have shown that the small, equiaxial grains are cubic SiC, whereas the plate-like grains are hexagonal.[4]

A dispersion of metallic-appearing second phase particles was observed in all the dense specimens.** Clear resolution of these second

*At 1980°C, the equilibrium Si vapor pressure over SiC is 10^{-1} Torr.[3]

**Specimen sintered with $\geq$ 6 w/o B were too friable for sectioning and observation.

phase particles could only be obtained for specimens which underwent extensive grain growth. As shown in Fig. 2, the second phase appeared to have been a liquid at the sintering temperature. Area and line scans for Si, C and B with an electron microprobe showed that these metallic-appearing second phase areas were enriched with B and depleted of Si relative to the surrounding SiC matrix. Some of these second phase areas were depleted of C, while others exhibited no changes. Prochazka and Scanlan[5] have also observed a uniform dispersion of B-rich inclusions using neutron activation, autoradiography techniques. C-rich inclusions which did not correspond to the metallic-appearing particles were also observed.

The microstructural observations strongly suggest that a B-rich liquid was present during densification. The extensive Si-B-C phase equilibrium work of Kieffer and coworkers[6] shows that only the SiC-SiB_6-Si compatibility triangle contains liquidus temperatures < 2100°C; the lowest eutectic temperatures in this compatibility triangle is 1380°C (~20 mole/o Si, ~80 mole/o B). These authors also found that Si and B_4C powder compositions react to form SiC with traces of SiB_6 obse microscopic examination.

Contrary to the hypothesis reported by Prochazka,[1,5] the observations presented here suggest that either reaction sintering or liquid-phase sintering is responsible for the densification of SiC + B compound compositions. Free Si, which is necessary for the occurrence of these phenomena, is available at high temperatures due to the decomposition of SiC. The observed phenomena, e.g., weight loss at temperatures corresponding to densification, too much B, which would cause a shift away from the lower eutectic compositions and the morphology-composition observations of the second phase, are consistent with a reaction or liquid-phase sintering phenomena. This work suggest that a further understanding of the relations between phase equilibria, reaction kinetics and atmospheric conditions might be useful for understanding the sintering phenomenon of SiC and other covalently bonded ceramics.

REFERENCES

1. S. Prochazka, "Sintering of SiC," Ceramics for High Performance Applications, ed. by J. J. Burk, A. E. Gorum and R. N. Katz, Book Hill Pub., Chestnut Hill, MA (1974).

2. F. F. Lange, "Hot-Pressing Behavior of SiC Powders with Additions of Al_2O_3," J. Mat. Sci. 10, 314 (1975).

3. P. Grieveson and C. B. Alcock, "The Thermodynamics of Metal Silicides and SiC," Special Ceramics 1, Ed. by P. Popper, pp. 183-208, B.C.R.A., Newcastle (1960).

4. F. F. Lange, Naval Air Systems Command Contract N00019-72-C-0278, Final Report, April 15, 1972.

5. S. Prochazka and R. M. Scanlan, "Effect of B and C on Sintering of SiC," J. Amer. Ceram. Soc. 58 [1-2], 72 (1975).

6. Von R. Kieffer, E. Gugel, G. Leimer and P. E. Honayer, "Untersuchungen im System Bor-Kohlenstoff-Silicium," Ber. Dt. Keram. Ges. 49 [2] 41-46 (1972; NBS SP 364, Solid State Chem., 505 (1972).

ACKNOWLEDGEMENTS

This work was supported by the Advanced Research Projects Agency and monitored by the Office of Naval Research under Contract N00014-74-C-0284.

Curve 684477-A

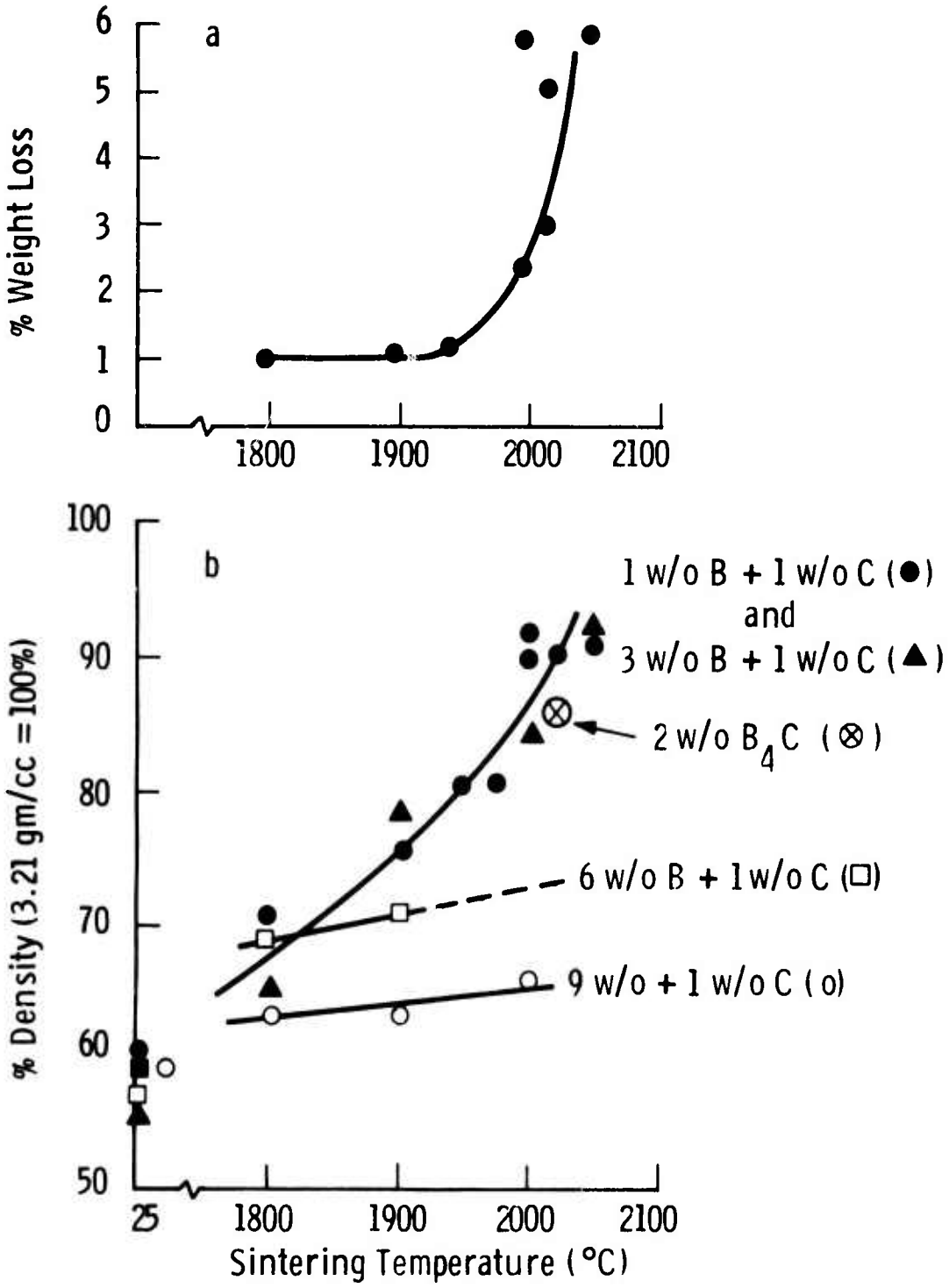

FIG. 1 -- a) % weight loss of SiC (1 w/o B + 1 w/o C) specimens sintered for 30 minutes vs temperature; b) % density (100% = 3.21 gm/cc) of various SiC-additions sintered for 30 minutes vs temperature.

FIG. 2 -- Polished surface of SiC + 2 w/o B_4C specimen sintered at 2020°C for 60 minutes showing the bright, metallic-appearing second phase areas rich in B and depleted in Si. Darker areas are holes due presumably to the pull-out of second phase particles (see arrows). Etching results (not shown) showed that the large plate-like grains contained pores (or removed second phase inclusions).